

The Measurement Method of Meat Conductivity

ZDENĚK BOHUSLÁVEK*

*Department of Electrical Engineering and Automation, Faculty of Engineering,
Czech University of Life Sciences in Prague, Prague, Czech Republic*

**Corresponding author: bohuslavek@tf.czu.cz*

Abstract

Bohuslávka Z. (2018): The measurement method of meat conductivity. Czech J. Food Sci., 36: 372–377.

This paper analyses the properties of electrode methods and contactless inductive methods of the conductivity measurement of biological tissue, which are one of the few which are able to measure the potentials of corresponding components of complex conductivity, i.e. the real reactive conductivity of a resistive and an imaginary component. The analysis was performed by computer modelling and experimental measurements. The publication describes the modelling of currents and of the potential by electrode and methods on tissue phantoms using the finite element method. The Comsol Multiphysics v3.4 program was used for the calculations. The results are presented in 2D and 3D diagrams. Experimental measurements with electrodes in phantom tissues with different conductivity were also conducted and the components of the complex conductivity were evaluated with an RLC Bridge and most accurately by using a lock-in amplifier. Results and experience from the experiments will make it possible to proceed with the next phase of research focused on measuring conductivity and dielectric properties in different types of meat.

Keywords: biological tissue; conductivity; contactless inductive methods; electrode method; meat; 2D and 3D diagrams

The quality and safety of meat can be determined with high precision by conductivity monitoring of a biological tissue. In addition, the components of complex conductivity can be used for monitoring the beef maturity level during the maturation in a cold storage, and the meat composition in terms of muscle and fat.

The intercellular environment conductivity and that of cytoplasm is approximately identical, and they vary in the range from 0.2 to 10 S/m. On contrary, the cell membranes conductivity is 10^6 – 10^8 times lower, i.e. about 1×10^{-6} to 10^{-8} S/m. The biological tissue can be massively present in the form of a suspension (mixture) of cells in an interstitial fluid, which appears in the dc field as a suspension of non-conductive elements in an electrolyte solution (Hrazdira & MORNSTEIN 2001; LIU *et.al.* 2017). In the simplified model of biological tissue, two types of electrical conductivity can be distinguished. The cytoplasm of cells and the tissue intercellular envi-

ronment behave like second order conductors, which are characterized by frequency-independent ohmic resistance, i.e. resistance (R). Due to specific capacitive properties, the membranes of biological tissue cells are therefore characterized by impedance (Z), in which in addition to resistance (R) also capacitance X_c asserts its effect (Equation 1) (HRAZDIRA & MORNSTEIN 2001):

$$Z = \sqrt{R^2 - X_c^2} \quad (\Omega) \quad (1)$$

where: Z – impedance; R – resistance; X_c – capacitive reactance

Based on these facts, the electrical properties of biological tissue in an alternating electric field can be assessed in two aspects. The complex permittivity is assessed from the aspect of dielectric properties and complex conductivity from the aspect of conductive properties. The permittivity of biological tissue in a complex form is described by Equation (2).

Supported by Czech University of Life Sciences in Prague, Faculty of Engineering, Grant IGA2015.

<https://doi.org/10.17221/164/2018-CJFS>

$$\varepsilon = \varepsilon_0 \varepsilon_r = \varepsilon_0 (\varepsilon_r' - j \varepsilon_r'') = \varepsilon_0 (\varepsilon_r' - j \frac{\sigma}{\omega \varepsilon_0}) \quad (\text{F/m}) \quad (2)$$

where: ε_0 – permittivity of vacuum; ε_r – complex relative permittivity; ε_r' and ε_r'' – real and imaginary part of the complex relative permittivity; j – imaginary unit; i.e. $j^2 = -1$; σ – electrical conductivity of the tissue; ω – angular frequency, i.e. $\omega = 2\pi f$; f – frequency of the alternating field

The conductivity of biological tissue can therefore be expressed in the formula (3):

$$\sigma = 2\pi f \varepsilon_0 \varepsilon_r'' \quad (\text{S/m}) \quad (3)$$

In biological tissue, the electric field causes polarization of ions, atoms and molecules. Besides this it also causes the rotation of the molecules bound to dipoles. As a result of these phenomena a current, the density J_v of which is given by Equation (4) is generated in biological tissue.

$$J_v = \sigma E = 2\pi f \varepsilon_0 \varepsilon_r'' E \quad (\text{A/m}^2) \quad (4)$$

In addition, a displacement current J_0 , also called capacitive current is generated the density of which can be expressed by Equation (5):

$$J_0 = \frac{\varepsilon_0 \varepsilon_r' \sigma E}{\sigma t} = 2\pi f \varepsilon_0 \varepsilon_r' E \quad (\text{A/m}^2) \quad (5)$$

The current of real conductive and capacitive components can be measured by electrode methods, and after the conversion of resistance and capacitance (reactance) of complex conductivity, it can be assessed. Contact methods are the simplest way of measuring the conductivity of biological tissue. The basic methods are a two- and a four-electrode method and methods of electrical impedance tomography. The simplest method for measuring conductivity is the two-electrode (bipolar) measuring method. This method uses two electrodes for both the excitation of electric current I in the circuit and measurement of the voltage U between the two electrodes see Figure 1A. The resulting resistance R is given by the sum of the resistance of the tissue sample, R -sample, and the parasitic resistances $R1$ el-sample and $R2$ el-sample. These parasitic resistances are undesirable and due to polarization or formation of deposits on the electrodes arising (PRANCE *et al.* 2000; OPEKAR 2002; OPPL 2002; CHI *et al.* 2010; HAQUE *et al.* 2015).

One way how to avoid this phenomenon is to generate a zero current in the measuring circuit, which can be achieved by applying the four-electrode measurement method. In the four-electrode measurement,

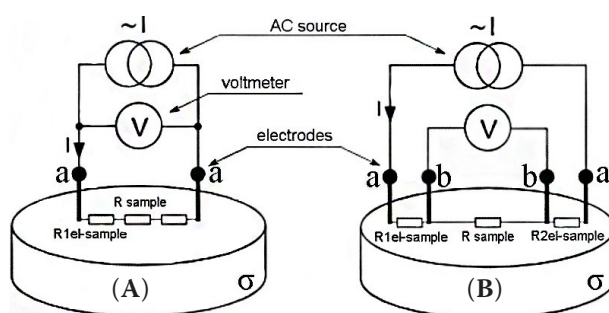


Figure 1. Electrode measurements of conductivity: (A) two-electrode method; (B) four-electrode method

the current I is flowing through two outer current (injection) electrodes and the voltage U is measured by a vector voltmeter connected to the inner two measuring (voltage) electrodes (Figure 1B). Due to the high input resistance of the voltmeter an almost zero current flows through the electrodes, and therefore the resulting resistance R is not affected by the parasitic resistances and electrode polarization as stated in (YAMASHITA 1989; GRISS *et al.* 2002; SCHUETZE 2004; HRUŠKA 2007; JI *et al.* 2014; JEON *et al.* 2017).

The content and object of the paper is to analyse the properties of the electrode conductivity measurement methods of complex biological tissues. The analysis was performed by computer modelling and experimental measurements. The publication describes the modelling current and potential electrode methods for tissue phantoms using the finite element method. The specific calculation program used was Comsol Multiphysics v3.4. The results are presented in 2D and 3D diagrams. Experimental measurements with electrodes were also performed on tissue phantoms with different conductivity, and the evaluation of the components of the complex conductivity was made using an RLC bridge and accurately by the use of a lock-in amplifier. The measured values were used as reference values for contactless measurement of conductivity.

MATERIAL AND METHODS

Measuring phantoms. Due to cost savings physical models were implemented in the initial tests of the measurement of conductivity of biological tissues referred to as tests of the measurement of phantoms.

Agar or gelatin can be used for simulating biological tissue with high water content such as the muscle tissue. A combination of various ingredients such as sodium chloride (NaCl) or aluminium powder can

change the dielectric parameters of the phantoms to meet those of the tissue in (ENDO *et al.* 2015; HAQUE *et al.* 2015).

For the initial test, a set of phantom homogenates were created, which simulate biological tissues in terms of the electrical conductivity σ . In order to prolong the life of the phantoms, the edible gelatin was used for their production. The values of conductivity of the phantoms were in the range: 3.7, 6.7, 10.3, 32, and 66.7 mS/cm.

Comsol Multiphysics. Comsol Multiphysics was applied to simulate and solve multi-physical tasks described by partial differential equations using the finite element method (FEM). Process modelling in Comsol Multiphysics consists of the following basic steps outlined in Comsol Multiphysics Humusoft. In our case, the Comsol Multiphysics program is used to simulate the distribution of the electric field in two and four-electrode conductivity measurements of biological tissue. In both cases, the same virtual model phantom with the identical conductivity and geometric dimensions was used. The geometric dimensions have been corresponding to the dimensions of real phantoms, i.e. $11 \times 11 \times 3$ cm. The value of conductivity selected for the virtual phantom was $\sigma = 4$ mS/cm, this conductivity value is corresponding to a healthy biological tissue.

The dimensions of the electrodes and their arrangement are identical to those during the real measurements. The selected supply voltage, which leads to the synoptic arrangement of the resulting graphs, was 1V CAD, Autodesk Inventor Professional 2010 was used in the creation of models of the electrodes and of the phantoms.

Conductivity measurement using electrodes. An EV-meter was used in the two-electrode measurement method for measuring the conductivity of meat. This device allows measuring the conductivity directly without any conversion, within the range 1–20 mS/cm. For the four-electrode method, a bridge of Escort ELC133A RLC type was used, it allows direct connection of the current (injection) and voltage (measuring) electrodes, making possible the measuring of the impedance Z and of the phase angle.

The buffer solutions of values 450, 4 500, and 45 000 $\mu\text{S/cm}$ were used for the calibration of the four-electrode method with an RLC bridge. Calibration of the two-electrode method with an EV-meter was made for the first two values only. The calibration was carried out at the frequency of 10 kHz, on which all measurements were made.

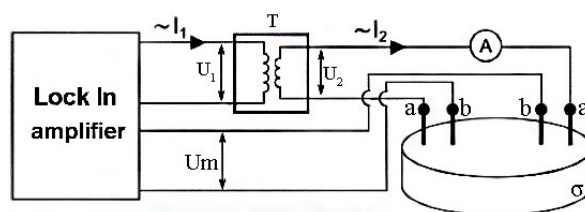


Figure 2. Block diagram of the four-electrode measurement method with a lock-in amplifier

The four-electrode method using a lock-in amplifier was designed and implemented for the measurement of contact conductivity. For measuring with four electrodes using RLC bridge, electrodes having an active surface area of 10, 15, and 1 mm were used. The electrodes were mounted side by side in a Plexiglas holder at a distance of 1, 4, and 1 cm. With this placement, the conductivity constant $K = 360$ mS/ Ω/cm was measured on the calibrated solutions. The inactive surfaces of the electrodes were coated with insulating material and thus did not influence the different depth of immersion. Of course, the condition was complete immersion to the uninsulated area had to be fulfilled. The lock-in amplifier makes it possible measuring the voltage U_m on the measuring electrodes only. The Figure 2 shows the block diagram of the proposed method of the four-electrode conductivity measurement of tissue, using a lock-in amplifier.

Conductivity measurement using contactless inductive method. Contactless inductive methods use various arrangements of two or three coils.

(1) For example two coils can be located above each other or side by side—one in (AHMAD & GENCER 2001; RIEDEL *et al.* 2004), the primary coil, is supplied from an alternating voltage generator and the second, secondary coil, generates voltage affected by the conductivity of the matter applied to this coil at a constant distance. The analysed matter must have the same dimensions and therefore also the same volume (GENCER & TEK 2006).

(2) The three-coil arrangement is implemented in the form of differential connection of coils. This is more appropriate from the aspect of resistance against interferences (temperature, electromagnetic interference, etc.) and appropriate for subsequent evaluation by measuring amplifiers. The diagram in Figure 3 shows a typical 3-coil arrangement was borrowed from paper (SAINT-GEORGE *et al.* 2002). On the basis of information from this publication a 3-coil sensor was designed with which the inductive measurements described below were carried out.

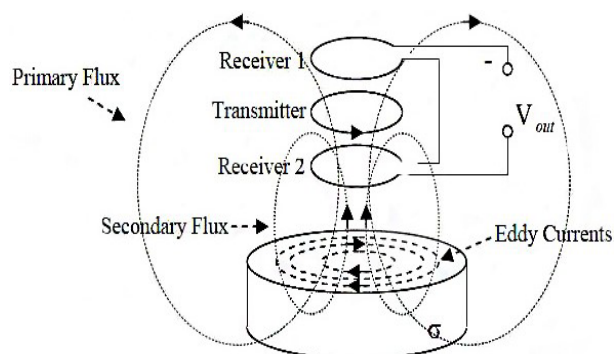


Figure 3. A differential coil sensor to measure body conductivity by sensing magnetic fields of induced eddy currents

In this method, magnetic excitation is used to induce eddy currents inside the body and the resulting magnetic fields are measured with pick up (receiver) coils. Primary flux generated by the transmitter coil induces eddy currents in the conductive object. Primary flux linked through the identical receiver coil is equal since both coils are at same distance from the transmitter coil which is the source of the primary field. However, secondary flux generated by the eddy currents flowing in the conductive object is linked through the differentially connected receiver coils unequally or in an unbalanced fashion due to the

fact that flux strength is diminished with distance. This causes a gradient in the receiver coils due to conductive object (Figure 3).

RESULTS AND DISCUSSION

(1) The results of the simulation of electrode measurements in the Comsol Multiphysics program are shown in Figure 4. The voltage between the electrodes is also represented by a gray scale in 3D.

The voltage non-linearity between the feeding electrodes is clearly apparent in the 2D view. These are electrodes in the two-electrode measurement method simultaneously measuring electrodes and therefore the value of the voltage between the electrodes can be erroneous. A change in the potential between the measuring electrodes in the four-electrode method is nearly linear. The electrodes in the graph are marked with an arrow at the locations of brief constant potential.

(2) The results of electrode measurements on homogeneous phantoms are illustrated in the bar chart in the Figure 5A which compares the results of the contact measurements. The structure of produced phantoms is homogeneous and therefore the capacitive component (reactance) was minimal.

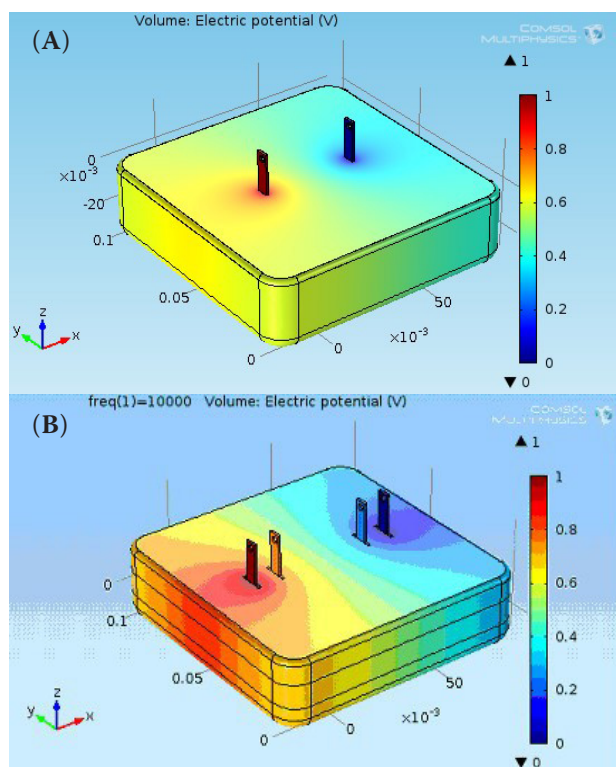
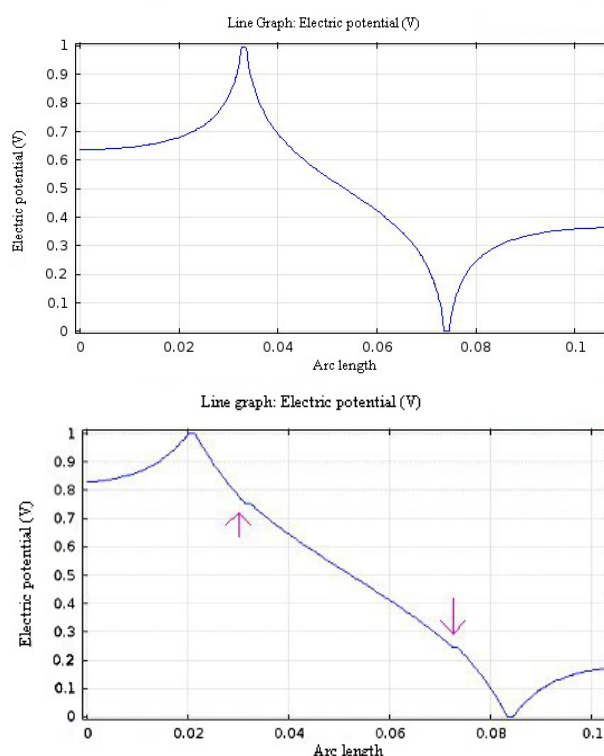


Figure 4. (A) The electric potential during the four-electrode measurement and (B) electric potential during the two-electrode measurement



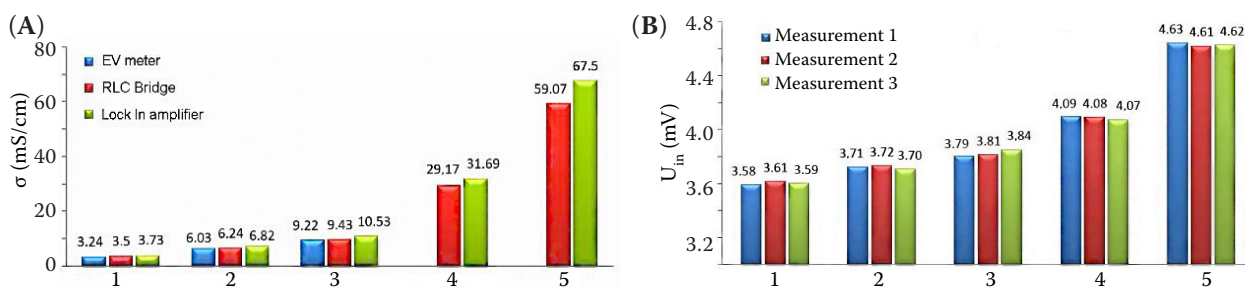


Figure 5. Comparison of contact measurements (A) and contactless measurements (B) on test phantoms

For these reasons only, the resistance was evaluated and the real conductivity subsequently calculated. The diagram shows that various contact methods can give similar values. The method with the lock-in amplifier gives the lowest deviations.

Minor deviations were caused by the inaccuracy of individual measurements due to inaccurate readings and due to small temperature changes and calibration inaccuracies. Owing to the smaller scale span of the measuring device, the measurements using the two-electrode method with an EV-meter were conducted only with the first three test phantoms with low conductivity. The conductivity of meat was measured in those cases when the sufficient upper limit of the measuring range was 20 mS/cm.

(2) The results of contactless measurements. The measurements were performed on testing phantoms. During contactless measurement on phantoms the inductive sensor was placed at a distance of 1 mm from the surface of the measuring phantoms. The difference in the measured values of U_{in} for individual phantoms was relatively small (Figure 5B). The measurements showed that the results were affected by the motion of metallic objects within a distance of 20 cm around the sensor.

CONCLUSIONS

The results of the study show that the four-electrode method is more accurate than the two-electrode one. The Finite Element Method implemented in the Comsol program can successfully simulate and analyse the behaviour of the potential and of current flows in biological tissues. The creation was verified of gelatin phantoms as the first step towards the creation of phantoms with a heterogeneous structure simulating the real dielectric properties of cellular tissue. From the obtained results of the measurements it is apparent that the contactless measurement of inductivity can be

implemented in practice with relatively good results in spite of the fact that the designed sensor has lower sensitivity and resolution.

Results and experience from the experiments will make it possible to proceed with the next phase of research focused on contactless inductive methods of measuring properties of biological tissues mainly in different types of meat. Further research must eliminate effects of the environment, e.g. by shading the measuring sensor from all sides except the front facing the measured specimen. Further it is important to place the specimen on a sufficiently large bed in order to eliminate affection of the measurement by objects in the environment.

References

- Ahmad T., Gencer N.G. (2001): Development of data acquisition system for conductivity images of biological tissues via contactless measurements In: Proceeding of 23rd Annual EMBS International Conference, Oct 25–28, 2001, Istanbul, Turkey: 25–28.
- Chi Y.M., Jung T.P., Cauwenberghs G. (2010): Dry-contact and noncontact biopotential electrodes. *IEEE Reviews in Biomedical Engineering*, 3: 106–119.
- Endo Y., Tezuka Y., Saito K., Ito K. (2015): Dielectric properties and water contents of coagulated biological tissue by microwave heating. *IEICE Communications Express*, 4: 105–110.
- Gencer N.G., Tek M.N. (2006): Imaging tissue conductivity via contactless measurements: a feasibility study. *Turkish Journal of Electrically*, 6: 183–200.
- Griss P., Tolvanen-Laakso H.K., Meriläinen P., Stemme G. (2002): Characterization of micromachined spiked biopotential electrodes. *IEEE Transactions on Bio-medical Engineering*, 49: 597–604.
- Haque M.A., Sulong A.B., Rosli R.E., Majlan E.H., Shyuan L.K., Mashud M.A.A. (2015): Measurement of hydrogen ion conductivity through proton exchange membrane. In:

<https://doi.org/10.17221/164/2018-CJFS>

- 2015 IEEE International WIE Conference on Electrical and Computer Engineering, Dec 19–20, 2015, Dhaka, Bangladesh: 552–555.
- Hrazdírka I., Mornstein V. (2001): Medical Biophysics and instrumentation. 1st Ed. Brno, Neptun: 396.
- Hruška F. (2007): Sensors in Systems Informatics and Automation. 1st Ed. Zlin, University of Tomas Bata in Zlin.
- Jeon E., Choi S., Yeo K.-H., Park K.S., Rathod M.L., Lee J. (2017): Development of electrical conductivity measurement technology for key plant physiological information using microneedle sensor. *Journal of Micromechanics and Microengineering*, 27: 45–49.
- Ji H., Chang Y., Huang Z., Wang B., Li H. (2014): Voidage measurement of gas-liquid two-phase flow based on capacitively coupled contactless conductivity detection. *Flow Measurement and Instrumentation*, 40: 199–205.
- Liu Y., Yang X., Zhu Q., Ju P., Ishii M., Buchanan J. R. (2017): Development of the droplet-capable conductivity probe for measurement of liquid-dispersed two-phase flow. *International Journal of Multiphase Flow*, 88: 238–250.
- Opekar F. (2002): Conductometry and dielectrometry. Available at <http://web.natur.cuni.cz/~opekar/elchem-chzp/elanalchzp6.doc>
- Oppl L. (2002): Measurement of dielectric parameters of biological tissue. [Dissertation Thesis.] Prague, CVUT in Prague.
- Prance R.J., Debray A., Clark T.D., Prance H., Nock M., Harland C.J., Clippingdale A.J. (2000): An ultra-low-noise electrical-potential probe for human-body scanning. *Measurement Science and Technology*, 11: 291–297.
- Riedel C.H., Keppelen M., Nani S., Merges R.D., Dössel O. (2004): Planar system for magnetic induction conductivity measurement using a sensor matrix. *Physiological Measurement*, 25: 403–411.
- Saint-George M., Riedel C.H., Dössel O. (2002): Design of a system for contact free measurement of the conductivity of biological tissue. *Biomedizinische Technik*, 47: 794–797.
- Schuetze A.P. (2004): A laboratory on the four-point probe technique. *American Journal of Physics*, 72: 149–153.
- Yamashita M., Enjoji H. (1989): Resistivity correction factor for the four-circular-probe method. *Japanese Journal of Applied Physics*, 28: 258–263.

Received: 2018–06–05

Accepted after corrections: 2018–09–10